Int. J. Heat Mass Transfer. Vol. 6, pp. 33–48. Pergamon Press 1963. Printed in Great Britain.

MASS MINIMIZATION OF RADIATING TRAPEZOIDAL FINS WITH NEGLIGIBLE BASE CYLINDER INTERACTION†

B. V. KARLEKAR‡ and B. T. CHAO§
University of Illinois, Urbana, Illinois

(*Received* 22 *May* 1962 *and in revised form* 19 *July* 1962)

Abstract—An optimization procedure is presented for achieving maximum dissipation from a longitudinal fin system of trapezoidal profile with mutual irradiation. The fins are conceived to be arranged symmetrically around a small base cylinder of uniform temperature. The governing equation for the temperature field along the fin is formulated in terms of finite summation and differences. The resulting set of simultaneous, non-linear, algebraic equations was solved by iteration using the Newton–Raphson method.

A new dimensionless parameter is proposed to characterize the total dissipating capacity of a fin system with mutual irradiation. Its use has advantage over the conventional fin effectiveness in design application.

Trapezoidal fins, including triangular and rectangular profiles, were investigated for a wide range of emissivities and incident space radiation. Optimum fin number and their proportions were determined and charts of dissipation capacity were presented. This analysis also leads to an expression suitable for comparing performance of fin systems fabricated of materials of different conductivity and density. For a fixed total mass of the fin material, the maximum dissipation varies as the 1/3 power of the quantity k/ρ, other factors remain unaltered.

NOMENCLATURE

Any consistent system of units may be used; the engineering system is indicated below.

A_T, total profile area of the fin system, $(NLt_0/2)(2-\tau)$, ft²;

B, radiosity, radiant energy leaving a surface per unit time and area, Btu/h ft². B^* = dimensionless radiosity, $B/\sigma T_0^4$;

F, configuration factor. F_{ij} = configuration factor of the ith element with respect to the jth element. F_{is} = configuration factor of the ith element with respect to the imaginary surface S;

H, irradiation, incident radiant energy per unit time and area, Btu/h ft². H^* = dimensionless irradiation, $H/\sigma T_0^4$;

k, thermal conductivity, Btu/h ft degR;

L, fin height, ft;

M, total number of sub-divisions along the fin height; also, the number of non-linear, simultaneous equations;

N, fin number;

Q_T, total rate of dissipation of the fin system per unit axial length of the base cylinder, Btu/h ft;

r, reflectivity, r_e = reflectivity with respect to stellar radiation;

S, imaginary black surface joining the tips of two adjoining fins, ft²;

T, absolute temperature, degR. T_e = equivalent temperature of S, degR;

t, fin thickness, ft;

W_T, total mass of the fin system per unit axial length of the base cylinder, lb_m/ft.

Greek symbols

δ, angle between the central planes of two adjacent fins, $2\pi/N$ rad. δ_f = included angle between the surfaces of the trapezoidal fin,

$$\sim \frac{t_0 - t_M}{L} \text{ rad};$$

ξ, dimensionless dissipation parameter, $Q_T/(\sigma^2 T_0^3 k A_T)^{1/3}$;

† This paper is based partly on a Ph.D. Thesis by Karlekar [1].

‡ Formerly, Graduate Student, now of Baroda, India.

§ Professor, Department of Mechanical Engineering and of Nuclear Engineering University of Illinois, Urbana, Illinois.

ϵ, emissivity;
η, fin system effectiveness, defined by equation (14);
θ, dimensionless temperature, T/T_0;
λ, dimensionless parameter, $\sigma T_0 L^3 N(2-\tau)/kA_T$;
ρ, density, lb_m/ft^3;
σ, Stefan–Boltzmann constant, $= 0{\cdot}1713 \times 10^{-8}$ Btu/h ft^2 degR^4;
τ, aspect ratio, $1 - (t_M/t_0)$.

Subscripts

i, j, refer to the ith and jth sub-division;
M, refers to fin tip;
o, refers to fin root;
opt, optimum values.

INTRODUCTION

In recent years, interest in fins with radiation heat transfer has been stimulated by man's desire of space exploration. Radiation is almost the exclusive mechanism by which waste heat from power plants or other heat generating equipment in spacecrafts can be dissipated. It is obviously desirable to minimize the mass of fins used on space radiators. A survey of literature reveals that considerable amount of study has been devoted to the subject during the past 5 years. MacKay and Leventhal [2] reported a procedure of achieving optimization for a flat plate uniformly heated on one edge. Lieblein [3] presented results of rectangular fin efficiencies for various ratios of sink to source temperature. Bartas and Sellers [4] studied a heat rejecting system consisting of parallel tubes joined by web plates that served as extended surfaces. A relation was established giving the maximum rate of heat dissipation for a given weight. The solutions were obtained by numerical computation. An analytical solution of the same problem was given by Chen [5]. Callinan and Berggren [6] analysed rectangular fins attached to tubes having axial temperature gradient. Tatom [7] described a method of obtaining temperature distribution along a rod in the presence of solar radiation, and Chambers and Somers [8] had studied the efficiency of circular fins. Very recently, the condition of optimization for a rectangular fin taking into account the heat transfer at the tube surface was examined by Schreiber *et al.* [9].

Wilkins Jr. [10] and Nilson and Curry [11]gave expressions for the optimum proportion of triangular fins radiating to space at absolute zero. Wilkins Jr. [12] has also discovered a novel similarity transformation which eliminates the nonlinear differential equation of the temperature field and greatly simplifies the solution procedure. The optimum fin profile could be obtained for any arbitrary surface dissipation mechanism, either convective or radiative or both.

In all the papers cited above, consideration has been confined to fins which exchange heat with space but have no radiant interaction with adjacent fins. The necessity of considering mutual irradiation in fin system optimization has been pointed out by Eckert, Irvine Jr. and Sparrow [13]. These authors also gave a penetrating discussion of some important characteristics of radiating fins and presented a general mathematical formulation of the problem. In a subsequent paper by the same authors [14], computer results for effectiveness, temperature distribution and local heat loss for straight rectangular fins were presented. They also gave optimum proportions of the fin when the angle between two adjacent fins was independently specified.

Let us consider the conduction–radiation heat transfer process in longitudinal fins of trapezoidal profile, equally spaced around a long base cylinder of small diameter. For a fixed total mass of the fin system, it is conceivable that the total dissipation may be increased by increasing the number of fins, thus providing a larger area for surface dissipation. On the other hand, a larger fin number would result in a decrease of energy dissipation for the individual fin not only due to the decrease in effective radiation exchange with space but also due to a smaller area available for conduction. This suggests that the optimization procedure should be based on the total radiating capacity of the fin system as a whole, and thus necessitates the simultaneous determination of fin number and its proportion. It is pertinent that for a rectangular fin system radiating into space at zero absolute temperature, the said optimization condition could be evaluated using the information given in reference [14].

Theoretically speaking, the optimization of

any fin system requires also the determination of the cross-section profile. This undoubtedly would multiply the complexities of an already difficult problem, at least from the viewpoint of computation. For practical applications, this seldom has been found necessary since its performance is not expected to differ significantly from that of an optimized trapezoidal system. Even if the theoretical profile could be determined, fabrication difficulties would probably prevent its use.

ANALYSIS

Consideration is hereby given to plane, radiating fins of trapezoidal cross section equally spaced around a base cylinder whose radius is small relative to the fin height, L. See Fig. 1 (a). It is desired to determine the optimum fin number and proportions of such fins.

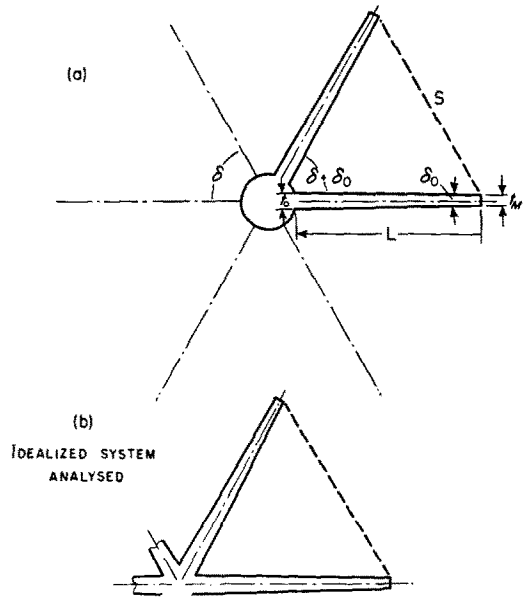

FIG. 1. Fin system configuration.

Assumptions

1. The fin material has a uniform conductivity and emissivity, both being independent of temperature. Its surface behaves like a diffuse emitter and reflector. The assumption of uniform material properties is introduced for convenience; the present analysis is equally adaptable to variable k and ϵ.
2. The fin system is long in the axial direction of the base cylinder and heat flow in that direction is negligible.
3. The individual fins are thin and hence the conduction heat flow is one-dimensional.
4. The thermal condition at the base cylinder is uniform, so is that of the external environment. The latter may be interpreted that the fin system has a rotation about the axis of the cylinder in the presence of incident solar radiation. This assumption preserves the symmetry of the problem; thus greatly simplifies the analysis.
5. Radiant interaction between the fin and the base cylinder is negligible. This is justifiable only when the base cylinder radius is small compared to fin height, L. Effects of mutual irradiation occurring between a single fin and its adjoining base surface have been examined by Sparrow and Eckert [15]. In conclusion, they remarked, "... for non-black surfaces, ... an extensive computing effort would be required to achieve numerical results. Such an undertaking would appear worth while only when application to a specific design is being considered." In this paper, we confine ourselves to a consideration of an idealized system as shown in Fig. 1 (b).

FINITE DIFFERENCE FORMULATION OF GOVERNING EQUATION OF TEMPERATURE FIELD IN THE FIN

Fig. 2 shows an enlarged view of two adjacent fins. Each is sub-divided into $M - 1$ elementary volumes of equal length Δx, but with half-length volumes at the root and at the tip. Under steady heat flow condition, application of the principle of energy conservation to the ith element leads to:

$$\frac{kt_0}{2\Delta x}\left[\left(1 - \frac{i}{M}\tau\right)\Delta^2 T_i + \frac{\tau}{M}\Delta T_i\right] = (B_i - H_i)\Delta x \quad (1)$$

for $i = 1, 2, \ldots, M$, the quantity $\Delta^2 T_i = T_{i-1} - 2T_i + T_{i+1}$ and $\Delta T_i = (T_{i-1} - T_{i+1})/2$. In (1), the left-hand side represents the net rate at which

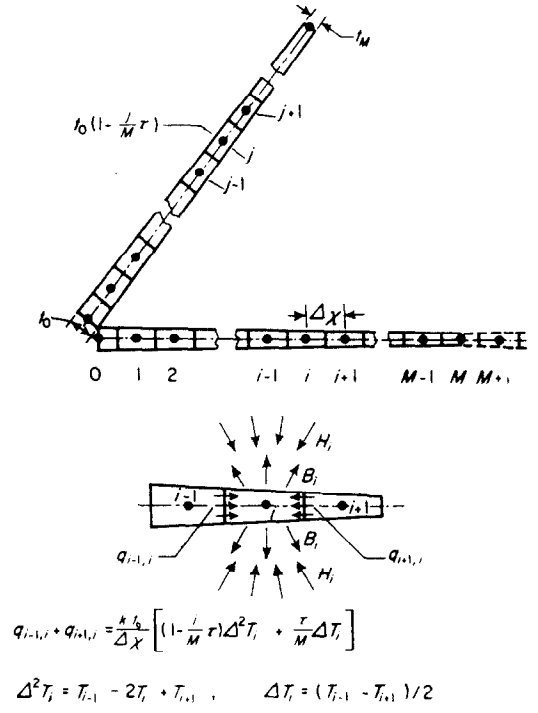

FIG. 2. Scheme of sub-division and energy balance for node i.

heat is flowing into the ith element by conduction; the right-hand side represents the net rate at which heat is leaving by radiation. The quantity $t_0[1 - (i/M)\tau]$ is the average thickness of the trapezoidal fin at the ith node. Due to symmetry, only one half of the fin thickness is considered.

The irradiation H_i consists of energies from two distinctive sources: (a) due to radiation leaving the adjacent fin surface, $H_i^{(1)}$, and (b) due to radiation from space or environment, $H_i^{(2)}$. The latter may be characterized by an equivalent radiation from an imaginary black surface S of uniform temperature T_e which connects the tips of the adjacent fins. Using the well known reciprocity relation of configuration factors for diffuse radiation, one finds,

$$H_i^{(1)} = \sum_{j=0}^{M} F_{ij}B_j, \quad i = 0, 1, \ldots, M \quad (2a)$$

$$H_i^{(2)} = \sigma T_e^4 F_{is}, \quad i = 0, 1, \ldots, M \quad (2b)$$

with

$$F_{ij} = \frac{ij\sin^2(\delta+\delta_f)}{2[i^2+j^2-2ij\cos(\delta+\delta_f)]^{3/2}}, \quad i \neq 0, j \neq 0 \quad (3a)$$

and

$$F_{is} = \frac{1}{2} - \frac{M\cos(\delta+\delta_f) - i}{2[i^2+M^2-2iM\cos(\delta+\delta_f)]^{1/2}}, \quad i = 0, 1, \ldots, M \quad (3b)$$

(3a) and (3b) were formulated from equations (31–58) in reference [16] together with the usual finite difference approximation. (3a) fails when $i = 0$ and/or $j = 0$. However, if one interprets F_{00} as the configuration factor between two long, identical strips of width $\Delta x/2$, having a common edge and an included angle of $\delta + \delta_f$, it can be shown that,

$$F_{00} = 1 - \left[\frac{1-\cos(\delta+\delta_f)}{2}\right]^{1/2}. \quad (3c)$$

Also, in subsequent numerical computations, F_{0j} (with $j = 1, 2 \ldots, M$) would be evaluated by setting $i = \frac{1}{4}$ in (3a). This means that for the half-length element at the fin root, the node is considered to be located not at the origin 0 but at the mid-point of that element.

For the radiosity, we may write,

$$B_i = \epsilon\sigma T_i^4 + rH_i^{(1)} + r_e H_i^{(2)}, \quad i = 0, 1, \ldots, M \quad (4)$$

in which r_e is the reflectivity of the fin surface with respect to space radiation. In general it is taken to be different from r, which is the reflectivity for radiation emanating from the adjoining fin. The latter is related to the emissivity by: $r = 1 - \epsilon$.

Eliminating $H_i^{(1)}$ from (1) and (4) yields,

$$B_i = \sigma T_i^4 + \frac{r_e - r}{\epsilon}\sigma T_e^4 F_{is} - \frac{r}{\epsilon}\frac{kt_0}{2(\Delta x)^2}\left[\left(1-\frac{i}{M}\tau\right)\Delta^2 T_i + \frac{\tau}{M}\Delta T_i\right] \quad (5)$$

which is valid for $i = 1, 2 \ldots, M$. Due to symmetry, one may obtain an expression for B_j by simply replacing i by j in the above equation.

When these results are substituted into (1) together with the relationships (2a) and (2b), followed by introducing the dimensionless parameters defined by:

$$\theta = \frac{T}{T_0}, \quad M = \frac{L}{\Delta x}, \quad F_{ij} = F_{ij} + \frac{rF_{i0}}{1 - rF_{00}} F_{0j} \tag{6a}$$

and

$$\lambda = \frac{\sigma T_0^3 L^3 (2 - \tau) N}{k A_T} = \frac{2\sigma T_0^3 L^2}{k t_0} \tag{6b}*$$

one obtains, after some rearrangement,

$$\left.\begin{aligned} &\theta_i^4 - \frac{1 - r_e}{\epsilon} F_{is}\theta_e^4 \\ &- \frac{M^2}{\epsilon\lambda}\left[\left(1 - \frac{i}{M}\tau\right)\Delta^2\theta_i + \frac{\tau}{M}\Delta\theta_i\right] \\ &- \frac{F_{i0}}{1 - rF_{00}}(\epsilon + r_e F_{0s}\theta_e^4) \\ &- \sum_{j=1}^{M}\left\{\theta_j^4 - \frac{rM^2}{\epsilon\lambda}\left[\left(1 - \frac{i}{M}\tau\right)\Delta^2\theta_j \right.\right. \\ &\left.\left. + \frac{\tau}{M}\Delta\theta_j\right] + \frac{r_e - r}{\epsilon} F_{js}\theta_e^4\right\} F_{ij} = 0 \end{aligned}\right\} \tag{7}$$

for $i = 1, 2 \ldots, M$. Here again $\Delta^2\theta_i = \theta_{i-1} - 2\theta_i + \theta_{i+1}$ and $\Delta\theta_i = (\theta_{i-1} - \theta_{i+1})/2$. We note that the two end conditions are, $\theta_0 = 1$ and $\theta_{M+1} = \theta_{M-1}$. The former corresponds to the uniform root temperature T_0 while the latter arises from the stipulation that heat loss at the fin tip is negligible.

Equation (7) is presented in a form convenient for machine computation. It constitutes a set of simultaneous non-linear, algebraic equations of M unknowns, namely, $\theta_1, \theta_2 \ldots, \theta_M$. The solution is seen to depend on six parameters θ_e, ϵ, r_e, τ, λ and N (or δ, which appears in the expression for configuration factors). In many design problems the quantities θ_e, ϵ, r_e and τ are either given or specified. Thus, the optimization of the fin system reduces to the problem of determining λ and N to achieve maximum dissipation for a given total mass.

Alternate formulations of the equation set (7) based on the governing integro-differential equation for the temperature field along the fin and on the electric network analog are separately given in Appendix A and B.

SOLUTION OF SIMULTANEOUS, NON-LINEAR, ALGEBRAIC EQUATIONS

In the literature, extensive information is available for solving simultaneous, linear, algebraic equations [17]. In contrast, only a meagre amount of work has been done when the equations are non-linear. The several methods of solution [18–21], which the authors are aware of, are all iterative in nature, although they differ in detail. A principal factor governing the selection of solution method for a particular category of problem is the rapidity with which a satisfactory solution can be obtained. Among other factors, this depends on the proximity of the initial guess to the exact solution, accuracy desired, the order of the interative process and the computer time required to generate a new set of iterates. It often happens that the last two factors counteract each other.

The Newton–Raphson method of iteration has been used throughout the present investigation. Earlier, the Gauss–Seidel iterative procedure modified for non-linear equations had also been examined but was later abandoned due to the longer overall computer time required to achieve the same degree of accuracy, starting with identical initial values of the unknowns. The general mathematical procedure of ascertaining the so-called "close enough" initial guess to guarantee convergence is of course difficult, but since the physical nature of the present problem can be readily apprehended, the task is not as hard as it appears. Indeed, our experience shows that so long as the initial θ's are selected positive and less than unity, the Newton–Raphson method converges for all the cases studied. While a detailed discussion of the method is beyond the scope of the paper, the success of obtaining results of the numerical computation actually hinges on the procedure. For this reason, a brief account of the Newton–Raphson method is presented in Appendix C.

* Parameter λ represents the ratio of surface conductance due to radiation to the internal conductance. It is analogous to Biot modulus commonly used in convective fin analysis.

HEAT DISSIPATION CAPACITY OF THE FIN SYSTEM

The total heat dissipation capacity of the fin system per unit axial length of the base cylinder, Q_T, may be computed from (i) the temperature gradient at the fin root, or (ii) net radiation over the fin surface. The latter is preferred since the truncation error associated with the finite difference approximation therein is of the second order. Hence,

$$Q_T = N\left[(B_0 - H_0) + 2\sum_{i=1}^{M-1}(B_i - H_i) + (B_M - H_M)\right]\Delta x. \quad (8)$$

Introducing the dimensionless quantities,

$$B_i^* = \frac{B_i}{\sigma T_0^4}, \quad H_i^* = \frac{H_i}{\sigma T_0^4} \quad (9a)$$

$$\xi = \frac{Q_T}{(\sigma^2 T_0^9 k A_T)^{1/3}}. \quad (9b)$$

Equation (8) becomes,

$$\xi = \left[\frac{\lambda}{(2-\tau)N}\right]^{1/3}\frac{N}{M}\left[(B_0^* - H_0^*) + 2\sum_{i=1}^{M-1}(B_i^* - H_i^*) + (B_M^* - H_M^*)\right]. \quad (10)$$

The dimensionless dissipation parameter ξ as defined above does not contain the fin length, L, and is thus more suitable for the present optimization study than the seemingly simpler quantity $Q_T/\sigma T_0^4 L$. In (10), B_i^* is given by,

$$B_i^* = \theta_i^4 + \frac{r_e - r}{\epsilon}F_{is}\theta_e^4 - \frac{rM^2}{\epsilon\lambda}\left[\left(1 - \frac{i}{M}\tau\right)\Delta^2\theta_i + \frac{\tau}{M}\Delta\theta_i\right] \quad (11a)$$

for $i = 1, 2, \ldots, M$. It is simply a dimensionless version of (5). When all the θ_i's are known, computation of B_i^* becomes a straight-forward substitution. For B_0^*, use is made of (4) written for the case $i = 0$. After recasting in dimensionless form and some rearrangement, one gets

$$B_0^* = \frac{1}{1 - rF_{00}}(\epsilon + r\sum_{j=1}^{M}F_{0j}B_j^* + r_eF_{0s}\theta_e^4). \quad (11b)$$

Having thus obtained all the B_i^*'s, the H_i^*'s can be evaluated from the following relation:

$$\left.\begin{aligned} &H_i^* = H_i^{(1)*} + H_i^{(2)*} \\ &\text{with} \\ &H_i^{(1)*} = \sum_{j=0}^{M}F_{ij}B_j^* \\ &H_i^{(2)*} = F_{is}\theta_e^4 \end{aligned}\right\} \quad i = 0, 1, \ldots, M. \quad (12)$$

This completes the necessary relations for the calculation of ξ.

OPTIMIZATION PROCEDURE

Let W_T be the total mass of the fin system per unit axial length of the base cylinder, to be distributed equally among the N fins. It is a given, fixed quantity in our problem. Clearly, $W_T = \rho A_T$. We desire to determine the optimum number of fins and their proportion such that the heat dissipation capability is a maximum. To achieve this, the set of non-linear equations (7) is solved for different assigned values of λ keeping θ_e, ϵ, r_e, and N unchanged. This is followed immediately by an evaluation of the dissipation parameter ξ. All the $\xi - \lambda$ curves exhibit a maximum. The value of λ corresponding to this maximum ξ is designated as λ_{opt} which gives the optimum proportion for the fin number chosen. The maximum ξ obtained in this manner is a relative maximum since, for given θ_e, ϵ, r_e and τ, it varies with N. Hence the above procedure must be repeated for all conceivable values of N beginning with $N = 2$. The overall best distribution of the fin mass will be achieved when ξ attains an absolute maximum for the values of the parameters selected. The corresponding optimum fin number is designated as N_{opt}.

The above procedure is admittedly unsophisticated, but is simple, direct and actually practical. This is mainly due to the physical nature of the problem that the number of fins which could conceivably be arranged around the base cylinder is rather limited.

FIN EFFECTIVENESS

Following Sparrow, Eckert and Irvine Jr. [14], we define the effectiveness of the fin system, η, as the ratio of the actual heat loss to that of an

ideal system having identical geometry but with black surface and infinite thermal conductivity. Hence,

$$Q_{T,\text{ideal}} = 2NL\sigma(T_0^4 - T_e^4)\sin[(\delta + \delta_f)/2] \quad (13)$$

and

$$\eta = \frac{(B_0^* - H_0^*) + 2\sum_{i=1}^{M-1}(B_i^* - H_i^*) + (B_M^* - H_M^*)}{2M(1 - \theta_0^4)\sin[(\delta + \delta_f)/2]} = \left(\frac{2-\tau}{\lambda}\right)^{1/3} \frac{\xi}{2N^{2/3}(1 - \theta_e^4)\sin[(\delta + \delta_f)/2]} \quad (14)$$

which is also applicable for the individual fin. In practice, $\delta_f \ll \delta$ and may be ignored.

SELECTION OF FIN MATERIAL

One of the major concerns in the design of spacecraft is the minimization of the weight of the heat dissipating equipment. This naturally calls upon an examination of the performance of the optimum fin systems made of different material. To this end, we rearrange the expression for ξ as follows:

$$\frac{Q}{(\sigma^2 T_0^9 W_T)^{1/3}} = \left(\frac{k}{\rho}\right)^{1/3} \xi. \quad (15)$$

The dissipation parameter ξ for the optimized system $\xi_{\max,\text{opt}}$ is uniquely determined when the quantities θ_e, ϵ, r_e and τ are specified. In design, the fin root temperature T_0 and the amount of heat to be dissipated, Q_T, are usually known. Equation (15) thus indicates that a material possessing the largest values of k/ρ would provide the least mass. For a specified dissipation capacity, the mass of an optimized system varies directly with the density and inversely with the thermal conductivity of the fin material. This finding is formally identical to that for convective fins of optimum proportion.

RESULTS AND DISCUSSION

As noted earlier, the temperature distribution along the fin and the dissipation capacity of the system depend upon the parameter λ for specified values of θ_e, ϵ, r_e, τ and N. Table 1 lists the ranges of the values of these quantities used in the present investigation.

Table 1

θ_e	0, 0·25, 0·50
ϵ	0·50, 0·75, 0·90, 1·00
r_e	0·80
τ	0, 0·75, 0·99
N	2, 3, 4, 5, 6, 7, 8, 9, 10

The case $\theta_e = 0$ refers to space environment at absolute zero temperature. The other two values of θ_e correspond to an incident black radiation of 400 Btu/h ft² when the fin root temperatures are respectively at 2780°R and 1390°R. Since the fin system is conceived for dissipation of heat, it seems pertinent that relatively high values of emissivity need to be considered. The value of the reflectivity selected for space radiation is arbitrary, but it is believed to be representative of the one encountered in practice. Its effect comes into play only when $\theta_e \neq 0$. The three chosen values of the aspect ratio, τ, incorporate the limiting cases of rectangular and almost triangular fin section. The fin number ranges from 2 to 10 which encompasses the optimum configurations for the values of θ_e, ϵ, r_e and τ listed

The number of sub-divisions, M, was chosen to be sixteen. It gave satisfactory accuracy and required moderate machine computation time. All calculations were done on the "Illiac", the digital computer at the University of Illinois. The iteration process for solving the equation set (7) was allowed to continue till the largest absolute value of the increment as defined in equation (A.7) became equal to or smaller than 10^{-5}. Lowering this limit to 10^{-6} did not alter the computed value of ξ by more than 0·01 per cent but increased the machine time by 20 per cent.

Dissipation characteristics

Curves depicting the variation of ξ with λ for several values of τ, ϵ, θ_e and N are presented in Figs. 3–6*. All curves exhibit a maximum and a relatively gradual slope for $\lambda > \lambda_{\text{opt}}$. This is particularly true for low surface emissitivities.

* A complete set of sixteen curves is on deposit in the Mechanical Engineering Department, University of Illinois.

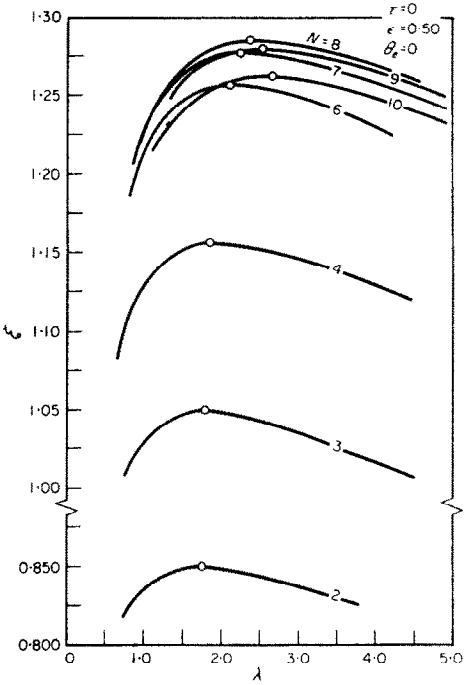

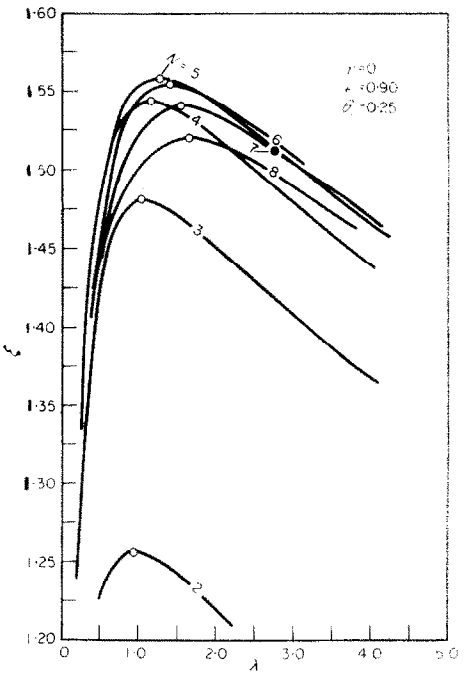

FIGS. 3, 4. Variation of ξ with λ. Rectangular profile.

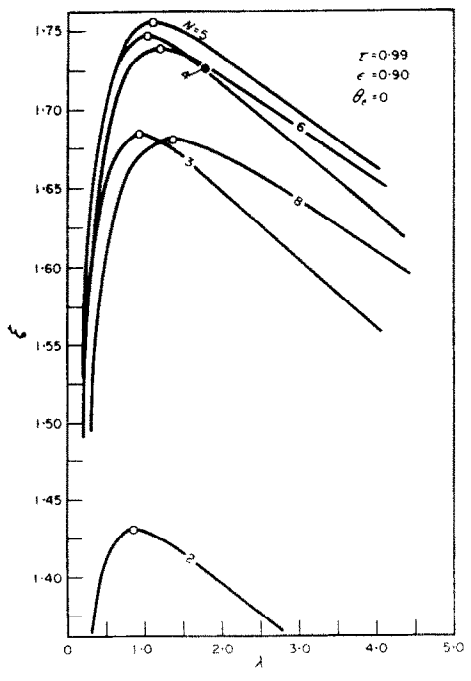

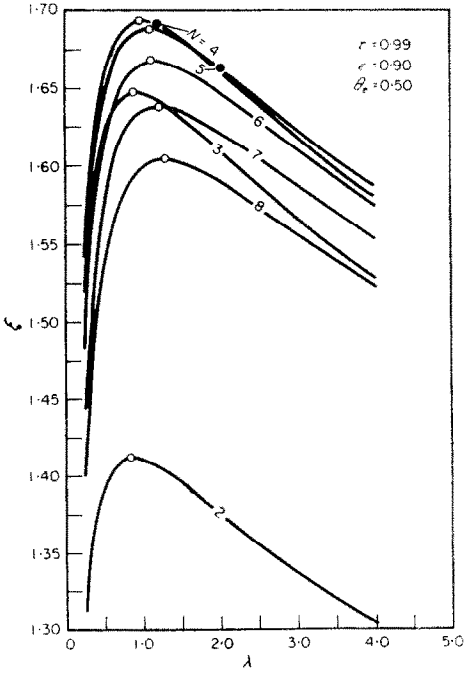

FIGS. 5, 6. Variation of ξ with λ. Triangular profile.

In design application, these curves are useful in that they provide for information on the reduction in dissipation capacity below the theoretical maximum if N_{opt} and λ_{opt} cannot be used due to structural or other reasons.

The case $N = 2$ corresponds to that without mutual irradiation, and hence the associated λ_{opt} gives also the optimum proportion of the individual fin. Reference [4] gave results for rectangular fins; while those for triangular fins were presented in [10] and [11]. The results obtained from the present analysis agree within 0·5 per cent with those reported therein. Other cases for which $\tau = 0$; $\theta_e = 0$; $\epsilon = 0{\cdot}50$, 0·75, 1·00 and $N = 3$, 4, 6, 8 have been investigated in [14]. The quantity N_c used in the latter reference corresponds to the parameter λ when $\tau = 0$. The values of λ_{opt} found from the present analysis agree with those of $(N_c)_{opt}$, within the reading accuracy of Fig. 5 in that reference.

Incident radiation has only minor effect on the heat dissipation capacity of the trapezoidal fin system, including the rectangular and triangular profiles, when $\theta_e = 0{\cdot}25$ or less. Some reduction is noticed, however, when $\theta_e = 0{\cdot}50$ (see Figs. 5 and 6). This is thought to be due to the high value of reflectivity assumed for stellar radiation.

As pointed out earlier, the dissipation parameter ξ for the optimum system is uniquely determined when θ_e, ϵ, r_e and τ are given. Table 2 summarizes the values of $\xi_{max,opt}$, N_{opt} and λ_{opt} for the ranges of parameters listed in Table 1.

The relative maximum values of ξ are shown plotted against the fin number for rectangular fins in Fig. 7 and triangular fins in Fig. 8, both with $\theta_e = 0$. It is seen that N_{opt} tends to increase with decreasing emissivity. Fig. 9 summarizes the result for $\epsilon = 0{\cdot}9$ but for several values of τ and θ_e.

The results of the present analysis demonstrate that the use of optimum number of fins could result in a substantial improvement of fin performance over the conventional two-fin system. Percentagewise, the improvement is 20·4, 24·2, 31·6 and 51·6 per cent for the rectangular case and 19·2, 23·0, 29·3 and 48·3 per cent for the almost triangular fin system. These values are for $\theta_e = 0$ and correspond to $\epsilon = 1{\cdot}00$, 0·90, 0·75 and 0·50 respectively. For a fixed emissivity of 0·90, the improvement amounts to 24·0 per cent when $\theta_e = 0{\cdot}25$ and 21·4 per cent when $\theta_e = 0{\cdot}50$ for the rectangular fins. The corresponding values for the triangular fins are 22·3 and 19·9 per cent. The advantage gained by optimizing the fin number as well as its proportion is, in general, quite impressive for low emissivities. For such an optimized system, the dissipation capacity always increases with

Table 2(a). ($\theta_e = 0$)

ϵ	$\tau = 0$			$\tau = 0{\cdot}75$			$\tau = 0{\cdot}99$		
	$\xi_{max,opt}$	N_{opt}	λ_{opt}	$\xi_{max,opt}$	N_{opt}	λ_{opt}	$\xi_{max,opt}$	N_{opt}	λ_{opt}
0·50	1·2850	8	2·35	—	—	—	1·4350	7	2·00
0·75	1·4690	6	1·58	—	—	—	1·6390	6	1·31
0·90	1·5620	5	1·28	1·6980	5	1·17	1·7563	5	1·15
1·00	1·6245	5	1·15	—	—	—	1·8310	4	0·95

Table 2(b) ($\epsilon = 0{\cdot}90$, $r_e = 0{\cdot}8$)

θ_e	$\tau = 0$			$\tau = 0{\cdot}99$		
	$\xi_{max,opt}$	N_{opt}	λ_{opt}	$\xi_{max,opt}$	N_{opt}	λ_{opt}
0·25	1·5585	5	1·27	1·7525	5	1·13
0·50	1·5040	5	1·25	1·6930	4	1·00

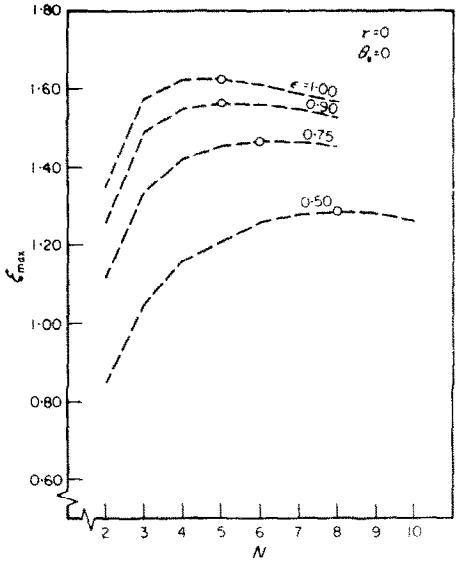

FIG. 7. Variation of ξ_{max} with N. Rectangular profile.

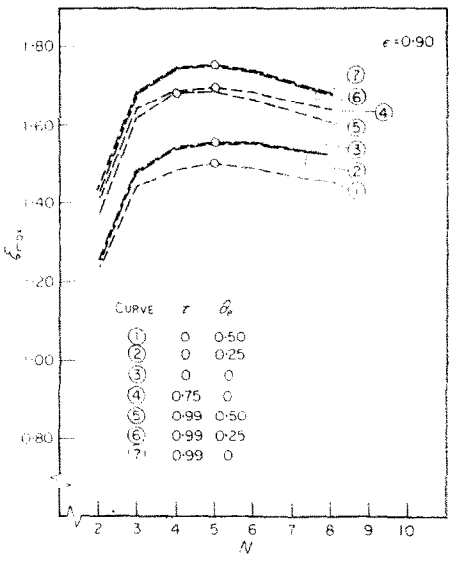

FIG. 9. Variation of ξ_{max} with N. (Note the relatively small influence of space radiation at low values of θ_p).

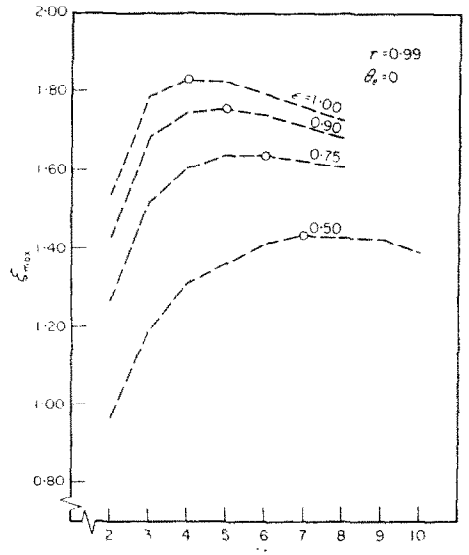

FIG. 8. Variation of ξ_{max} with N. Triangular profile.

an increase in emissivity and aspect ratio. The latter is to be expected since larger values of τ result in a better utilization of the fin material.

Optimum fin configuration

Variations of the quantity λ_{opt} with fin number are presented in Figs. 10 and 11. This parameter which characterizes the optimum fin proportion is seen to increase with a decrease in emissivity for a given N. This stems from the fact that when the emissivity is low, both the influence of mutual irradiation and the radiation exchange with space environment become less. To achieve optimization, a greater surface area and hence a longer fin is required to compensate for the reduction of radiant flux density. On the other hand, although λ_{opt} increases with N for a fixed ϵ, it does not follow that the optimum fin is longer when the fin number is greater. This becomes apparent when one realizes that λ is proportional to the product NL^3. Fig. 11 shows that incident stellar radiation has very minor effect on the λ_{opt}, while triangular fins exhibit a lower value.

Temperature distribution

Fig. 12 compares the computed temperature distribution along a triangular fin and two rectangular fins with published data. The agreement is excellent. The data taken from reference [11] are for the optimized, single, triangular fin, which is the same as the two-fin configuration considered in this analysis. The data obtained

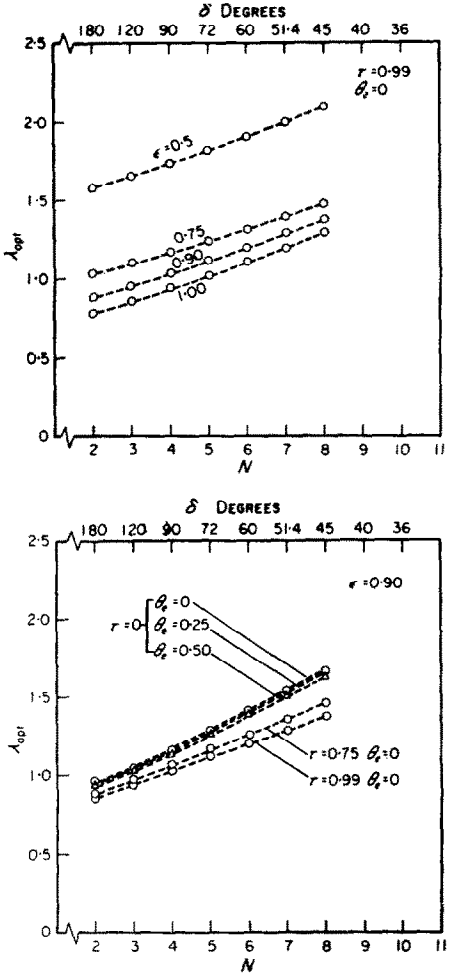

FIGS. 10, 11. Variation of λ_{opt} with N.

from reference [14] are not for the optimized systems. Under optimum conditions, the temperature distribution remains essentially unaltered over wide ranges of emissivity and incident radiation. This is shown in Fig. 13. On the other hand, changes in aspect ratio have a definite influence. As expected, a triangular fin has a steeper slope than the rectangular fin. The short, horizontal dotted line drawn through the fin tip at $x/L = 1$ emphasizes zero slope, although this may not be evident from the plot.

Fin effectiveness

One representative set of curves for fin effectiveness is shown in Fig. 14. Other sets covering the entire range of θ_e, ϵ, r_e and τ have also been calculated and are deposited at the authors institution. For optimization studies as well as in design application, the use of the parameter ξ is more convenient than fin effectiveness.

Performance of optimized fins of several materials

In order to compare the performance of optimized fin system fabricated of different materials, charts relating $Q_T/(\sigma^2 T_0^9 W_T)^{1/3}$ and $(k/\rho)^{1/3}$ are presented in Figs. 15 and 16 for aluminum, beryllium, copper and titanium at several temperatures. The values of thermal conductivity and density of these materials are taken from references [22] and [23]. These curves are evidently straight lines passing through origin having slopes equal to $\xi_{max,opt}$.

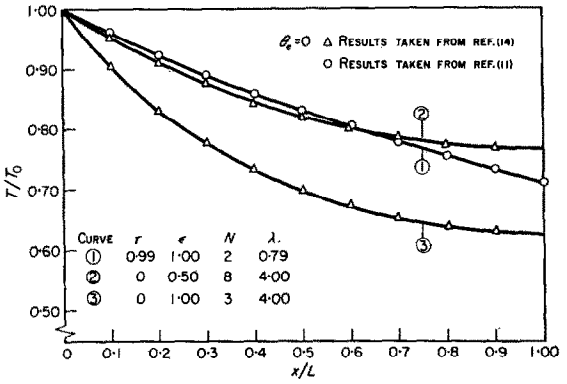

FIG. 12. Comparison of computed temperature distribution with data reported in references [11] and [14].

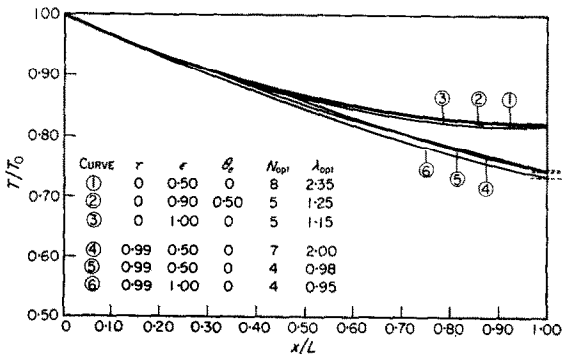

FIG. 13. Temperature distribution along fins of optimized systems.

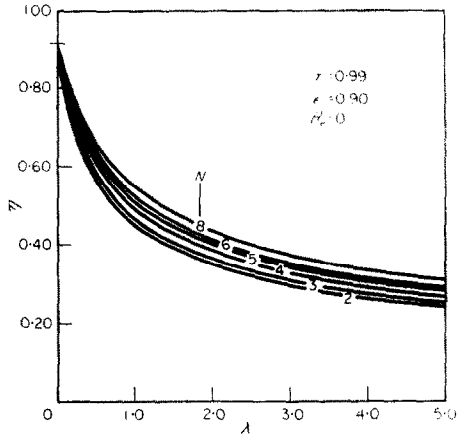

FIG. 14. Fin effectiveness.

Of the four materials, aluminum is the most desirable for high fin temperatures which are within its allowable operating limit. At 672°R, beryllium gives a slightly better performance. Quantitative application of these charts should be made with some caution, since, in the present analysis, possible variations of the thermal conductivity along the fin length due to temperature changes are not included.

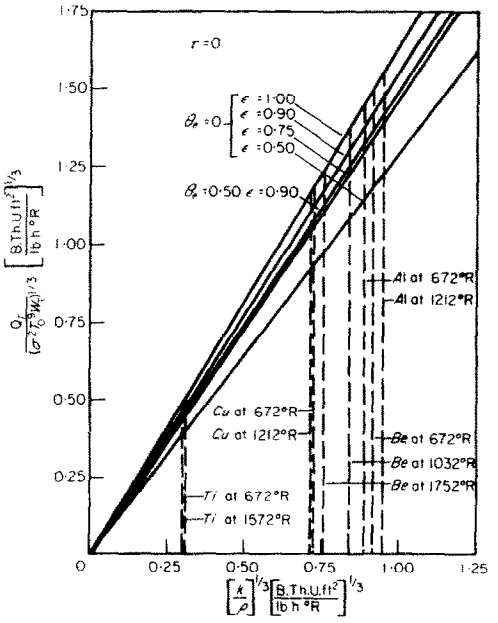

FIG. 15. Comparative performance of optimized fin Systems. Rectangular profile.

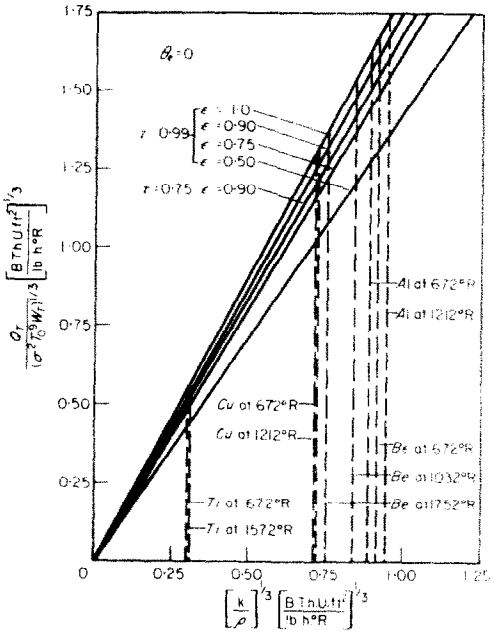

FIG. 16. Comparative performance of optimized fin systems. Trapezoidal and triangular profile.

CONCLUDING REMARKS

This analysis demonstrates the practicability and accuracy of using finite difference technique to study the optimization of radiation fin systems. The Newton–Raphson iterative procedure has been found superior to the modified Gauss–Seidel technique in solving the resulting non-linear, simultaneous, algebraic equations. Within the scope of this investigation, the method converges for any reasonable initial trial solution consistent with the physical nature of the problem. Due to the high flexibility inherent with the finite difference technique, problems involving variable properties, non-uniform incident radiation, exchange with base cylinder, etc. may be studied.

REFERENCES

1. B. V. KARLEKAR, Optimization of trapezoidal fin systems with mutual irradiation. University of Illinois, April (1962).
2. D. B. MACKAY and E. L. LEVENTHAL, Radiant heat transfer from a flat plate uniformly heated on one edge. Rep. MD 58-187, North American Aviation Inc., Calif. (1958).
3. S. LIEBLEIN, Analysis of temperature distribution and radiant heat transfer along a rectangular fin of constant thickness. *N.A.S.A.* TN D-196 (1959).

4. J. G. BARTAS and W. H. SELLERS, Radiation fin effectiveness, *Trans. ASME J. Heat Transfer*, **82**, 1, 73–75 (1960).
5. Y. L. CHEN, On minimum weight rectangular fins, *J. Aero. Space Sci.* **27**, 11, 871–872 (1960).
6. J. P. CALLINAN and W. P. BERGGREN, Some radiator design criteria for space vehicles, *Trans. ASME J. Heat Transfer*, **81**, 3, 237–244 (1959).
7. J. W. TATOM, Steady-state behavior of extended surfaces in space, *J. Amer. Rocket Soc.* **30**, 118–119 (1960)
8. R. L. CHAMBERS and E. V. SOMERS, Radiation fin efficiency for one dimensional heat flow in a circular fin, *Trans. ASME J. Heat Transfer* **81**, 4, 327–329 (1959).
9. L. H. SCHREIBER, R. P. MITCHELL, G. D. GILLESPIE and T. M. OLCOTT, Techniques for optimization of a finned-tube radiator. *ASME* Paper 61-SA-44, presented at the Summer Annual Meeting of the *ASME*, Los Angeles, Calif. (1961).
10. J. E. WILKINS, Jr., Minimizing the mass of thin radiating fins, *J. Aero. Space Sci.* **27**, 2, 145–146 (1960).
11. E. N. NILSON and R. CURRY, The minimum weight straight fin of triangular profile radiating to space, *J. Aero. Space Sci.* **27**, 2, 146–147 (1960).
12. J. E. WILKINS, Jr., Minimum mass thin fins for space radiators. *Proceedings of the* 1960 *Heat Transfer and Fluid Mechanics Institute, Stanford, Calif.*, 229–243 (1960).
13. E. R. G. ECKERT, T. F. IRVINE, Jr. and E. M. SPARROW, Analytic formulation for radiating fins with mutual irradiation, *J. Amer. Rocket Soc.* **30**, 7, 644–646 (1960).
14. E. M. SPARROW, E. R. G. ECKERT and T. F. IRVINE, Jr., The effectiveness of radiating fins with mutual irradiation, *J. Aero. Space Sci.* **28**, 10, 763–772 (1961).
15. E. M. SPARROW and E. R. G. ECKERT, Radiant interaction between fin and base surfaces, *Trans. ASME J. Heat Transfer* **84**, 1, 12–18 (1962).
16. M. JAKOB, *Heat Transfer*, Vol. 2, p. 19. John Wiley, New York (1957).
17. G. E. FORSYTHE, Tentative classification of methods and bibliography on solving system of linear equations. National Bureau of Standards, INA Report 52–7 (1951).
18. P. WOLFE, The secant method for simultaneous non-linear equations. *Communications of the Association for Computing Machinery* **2**, 12, 12–13 (1959).
19. M. SISLER, O Konvergenci Iteračních Metod Řešení Soustavy Nelineárních Rovnic (On the convergence of iterative methods for solution of non-linear, simultaneous equations). *Aplikace Matematiky*, No. 2, 141–150 (1960) (In Czechoslovak).
20. W. J. GOODEY, Note on the solution of non-linear simultaneous equations by successive approximation, *J. R. Aero. Soc.* **62**, 603–604 (1958).
21. A. J. NESS, Solution of equation of a thermal network on a digital computer, *Solar Energy*, **3**, 2, 37–38 (1959).
22. C. J. SMITHELLS, *Metals Reference Book*, 2nd Edition, Vol. II, pp. 636–639. Interscience Publishers, New York (1955).
23. E. R. G. ECKERT and R. M. DRAKE, Jr., *Heat and Mass Transfer*, 2nd Edition, pp. 496–499. McGraw-Hill, New York (1959).

APPENDIX A

Finite difference formulation from the integro-differential equation

Application of the law of energy conservation to a differential element of length $\mathrm{d}x$ of the trapezoidal fin shown in Fig. 2 leads to:

$$\frac{\mathrm{d}}{\mathrm{d}x}\left[k\frac{t(x)}{2}\frac{\mathrm{d}T(x)}{\mathrm{d}x}\right] = B(x) - H^{(1)}(x) - H^{(2)}(x) \tag{A.1}$$

where $t(x)$ is the fin thickness at a section distant x from 0. Its radiosity is,

$$B(x) = \epsilon\sigma T^4(x) + rH^{(1)}(x) + r_eH^{(2)}(x) \tag{A.2}$$

and the two distinctive sources of irradiation are,

$$H^{(1)}(x) = \int_0^L B(x')\,\mathrm{d}F_{xx'} \tag{A.3a}$$

$$H^{(2)}(x) = \sigma T_e^4 F_{xs}. \tag{A.3b}$$

Herewith the configuration factors $\mathrm{d}F_{xx'}$ and F_{xs} are given by:

$$\mathrm{d}F_{xx'} = \frac{xx'\sin^2(\delta+\delta_f)\,\mathrm{d}x'}{2[x^2+x'^2-2xx'\cos(\delta+\delta_f)]^{3/2}} \tag{A.4a}$$

$$F_{xs} = \tfrac{1}{2} - \frac{L\cos(\delta+\delta_f) - x}{2[x^2+L^2-2xL\cos(\delta+\delta_f)]^{1/2}}. \tag{A.4b}$$

Elimination of the quantities $B(x)$, $H^{(1)}(x)$ and $H^{(2)}(x)$ from (A.1), (A.2) and (A.3) results in the following non-linear integro-differential equation for the temperature field along the fin,

$$\sigma T^4 - \frac{1}{2\epsilon}\frac{\mathrm{d}}{\mathrm{d}x}\left(kt\frac{\mathrm{d}T}{\mathrm{d}x}\right) - \frac{1-r_e}{\epsilon}\sigma T_e^4 F_{xs} - \int_0^L \left\{\sigma T^4(x') - \frac{1-\epsilon}{2\epsilon}\frac{\mathrm{d}}{\mathrm{d}x'}\left[kt(x')\frac{\mathrm{d}T(x')}{\mathrm{d}x'}\right] + \frac{\epsilon-(1-r_e)}{\epsilon}\sigma T_e^4 F_{x's}\right\}\mathrm{d}F_{xx'} = 0, \tag{A.5}$$

The appropriate boundary conditions are $T(0) = T_0$ and $(dT/dx)(L) = 0$. By replacing the derivatives by difference quotients and integration by summation in the usual manner, one obtains the corresponding expression in finite differences and sums. In order to achieve a uniform approximation consistent with the use of central difference quotient for the second derivative, the quantity $(\Delta/\Delta x)[kt(\Delta T/\Delta x)]$ at origin is evaluated from the said finite difference expression for $i = 0$. Thus,

$$\left.\begin{aligned}\frac{1}{2\epsilon}\frac{\Delta}{\Delta x}\left(kt\frac{\Delta T}{\Delta x}\right)\Big|_0 = \frac{1}{1-rF_{00}}\Bigg\{&(1-F_{00})\sigma T_0^4 \\ &-\left[F_{00}+\frac{(1-r_e)(1-F_{00})}{\epsilon}\right]F_{0s}\sigma T_e^4 \\ &-\sum_{j=1}^{M}\left[\sigma T_j^4-\frac{1-\epsilon}{2\epsilon}\frac{\Delta}{\Delta x}\left(kt_j\frac{\Delta T_j}{\Delta x}\right)\right. \\ &\left.+\frac{\epsilon-(1-r_e)}{\epsilon}F_{js}\sigma T_e^4\right]\Bigg\}F_{0j}.\end{aligned}\right\}\quad(A.6)$$

Using this, one obtains the finite difference representation for (A.5) as follows:

$$\left.\begin{aligned}\sigma T_i^4-\frac{1-r_e}{\epsilon}F_{is}\sigma T_e^4-\frac{1}{2\epsilon}\frac{\Delta}{\Delta x}\left(kt_i\frac{\Delta T_i}{\Delta x}\right) \\ -\frac{F_{i0}}{1-rF_{00}}(\epsilon\sigma T_0^4+r_eF_{0s}\sigma T_e^4) \\ -\sum_{j=1}^{M}\left[\sigma T_j^4-\frac{1-\epsilon}{2\epsilon}\frac{\Delta}{\Delta x}\left(kt_j\frac{\Delta T_j}{\Delta x}\right)\right. \\ \left.+\frac{\epsilon-(1-r_e)}{\epsilon}F_{js}\sigma T_e^4\right] \\ \left(F_{ij}+\frac{rF_{i0}}{1-rF_{00}}F_{0j}\right)=0.\end{aligned}\right\}\quad(A.7)$$

Dividing each term of (A.7) by σT_0^4 and introducing the dimensionless quantities θ, M, τ, λ and $\bar{F}_{ij}$, one is immediately led to (7). The finite difference expressions for the configuration factors $dF_{xx'}$ and F_{xs} are obviously given by (3a) and (3b).

APPENDIX B

Derivation of equation (7) from the electric network analog

Fig. 17 illustrates an equivalent resistance network simulating the interplay between the geometrical and physical characteristics of the radiant exchange at the surface and the coupling between radiation and internal conduction along the fin. For clarity, only a portion of the network is shown. The internal nodes are designated by i and j, and the surface nodes by i' and j'. The various resistances and node potentials are as indicated.

Application of Kirchhoff's law to nodes i and i' leads respectively to:

$$\frac{E_i-E_{i+1}}{R_{i,i+1}}+\frac{E_i-E_{i-1}}{R_{i,i-1}}+\frac{E_i-B_i}{R_{i,i'}}=0\quad(B.1)$$

and

$$\frac{B_i-E_i}{R_{i,i'}}+\frac{B_i-E_s}{R_{i',s}}+\sum_{j=0}^{M}\frac{B_i-B_j}{R_{i',j'}}=0.\quad(B.2)$$

When the appropriate resistances are substituted into (B.2), one obtains after some rearrangement,

$$B_i=\epsilon E_i+r\sum_{j=0}^{M}F_{ij}B_j+r_eF_{is}E_s\quad(B.3)$$

wherein the summation relation for the configuration factors have been used. For the zeroth node, (B.3) becomes,

$$B_0=\frac{1}{1-rF_{00}}(\epsilon E_0+r\sum_{j=0}^{M}F_{0j}B_j+r_eF_{0s}E_s).\quad(B.4)$$

In a similar manner, we obtain from (B.1)

$$B_i=E_i-\frac{r}{\epsilon}\frac{kt_0}{2\sigma^{1/4}(\Delta x)^2}\times\left[\left(1-\frac{i}{M}\tau\right)(E_{i-1}^{1/4}-2E_i^{1/4}+E_{i+1}^{1/4})+\frac{\tau}{2M}(E_{i-1}^{1/4}-E_{i+1}^{1/4})\right]+\frac{r_e-r}{\epsilon}F_{is}E_s.\quad(B.5)$$

By writing j for i in (B.5), one obtains an expression for B_j. When these are substituted into (B.3), followed by introducing the dimensionless parameters defined in (6), one arrives at (7).

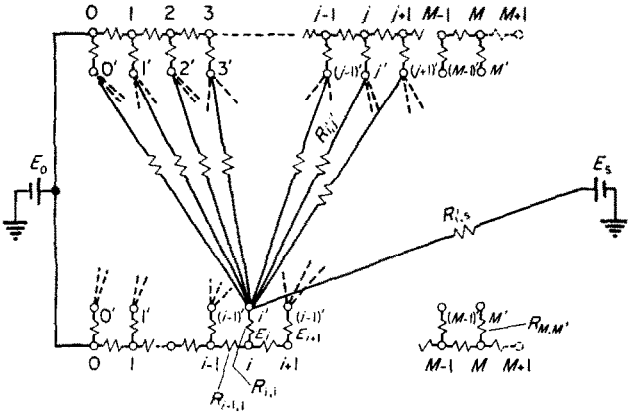

FIG. 17. Electrical network analog.

$$R_{i-1,i} = \left[\frac{kt_0}{2\Delta x}\,\frac{1-(\tau/M)(i-\frac{1}{2})}{\sigma^{1/4}(E_{i-1}^{3/4}+E_{i-1}^{1/2}E_i^{1/4}+E_{i-1}^{1/4}E_i^{1/2}+E_i^{3/4})}\right]^{-1}$$

$$R_{i,i'} = \left[\frac{\epsilon\Delta x}{1-\epsilon}+\frac{r_e-r}{1-\epsilon}\,\frac{E_s\Delta x}{E_i-E_{i'}}F_{is}\right]^{-1}$$

$$R_{i',j'} = (\Delta x F_{ij})^{-1}, \qquad R_{i',s} = (\Delta x F_{is})^{-1}$$

$$E_i = \sigma T_i^4,\ E_{i'} = B_i,\ E_0 = \sigma T_0^4,\ \text{and}\ E_s = \sigma T_e^4$$

APPENDIX C

The Newton–Raphson method

Let the set of non-linear equations be represented by,

$$\phi_i(\theta_1, \ldots, \theta_j, \ldots, \theta_M) = 0,\ i,j = 1, 2, \ldots, M. \tag{C.1}$$

In this method, the values of θ_j's of the $(\nu+1)$th iteration are determined from those of the νth cycle according to,

$$\theta_j^{\nu+1} = \theta_j^\nu + h_j^\nu, \quad \nu = 0, 1, \ldots \tag{C.2}$$

where the h_j^ν's are the solutions of the set of M linear, simultaneous equations prescribed by:

$$\phi_i(\theta_1^\nu, \ldots, \theta_j^\nu, \ldots, \theta_M^\nu) + \sum_{j=1}^{M} h_j^\nu \frac{\partial\phi_i^\nu}{\partial\theta_j} = 0. \tag{C.3}$$

The symbol $\partial\phi_i^\nu/\partial\theta_j$ signifies that the partial derivatives are to be evaluated at θ_j^ν's.

The Taylor series expansion of the function ϕ_i leads to,

$$\phi_i(\theta_1, \ldots, \theta_j, \ldots, \theta_M) = \phi_i(\theta_1^\nu, \ldots, \theta_j^\nu, \ldots, \theta_M^\nu) + \sum_{j=1}^{M} e_j^\nu \frac{\partial\phi_i^\nu}{\partial\theta_j} + \frac{1}{2!}\left(\sum_{j=1}^{M} e_j^\nu \frac{\partial}{\partial\theta_j}\right)^2 \phi_j^\nu + \text{terms of the order } (e_j^\nu)^3 \text{ and higher.} \tag{C.4}$$

In (C.4), e_j^ν stands for $(\theta_j - \theta_j^\nu)$ which is the error. From (C.2), we observe

$$e_j^\nu - e_j^{\nu+1} = h_j^\nu. \tag{C.5}$$

Substituting (C.5) into (C.4) and making use of (C.3), one obtains,

$$\sum_{j=1}^{M} e_j^{\nu+1} \frac{\partial\phi_j^\nu}{\partial\theta_j} + \frac{1}{2!}\left(\sum_{j=1}^{M} e_j^\nu \frac{\partial}{\partial\theta_j}\right)^2 \phi_i^\nu + \ldots = 0$$

which implies that the iteration is a second order process. This compares with the first order process of the Gauss–Seidel method.

Résumé—On présente un processus d'optimisation pour obtenir la dissipation maximum à partir d'un dispositif à ailettes longitudinales, à profil trapézoïdal, rayonnant les unes sur les autres. Les ailettes sont prévues pour un arrangement symétrique autour d'un petit cylindre à température uniforme. L'équation du champ de température le long d'une ailette est formulée en somme et différences finies.

Le système résultant d'équations algébriques non-linéaires est résolu par itération à l'aide de la méthode de Newton–Raphson.

On propose un nouveau paramètre sans dimensions pour caractériser la puissance de dissipation totale d'un dispositif d'ailettes à rayonnement mutuel. Dans les applications techniques leur utilisation est préférable à celle des ailettes conventionnelles les plus efficaces.

Les ailettes trapézoïdales et à profils triangulaires et rectangulaires ont été étudiées pour un large domaine de coefficients d'émission et de rayonnement incident. Le nombre d'ailettes optimum et leurs dimensions ont été déterminés et des diagrammes donnant leur puissance de dissipation sont présentés. Cette étude conduit également à une expression permettant de comparer les performances de systèmes d'ailettes faites à partir de matériaux de conductivité et de densité différentes. Pour une masse totale déterminée du matériau constituant les ailettes, la dissipation maximum varie comme $(k/\rho)^{1/3}$, les autres facteurs restent inchangés.

Zusammenfassung—Für die maximale Wärmeabgabe eines Systems von Längsrippen mit trapezförmigem Querschnitt bei gegenseitiger Zustrahlung wird ein Optimierungsverfahren angegeben. Die Rippen sollen symmetrisch an einem kleinen Zylinder von gleichmässiger Temperatur angebracht sein. Die für das Temperaturfeld längs der Rippe massgebliche Gleichung ist in Form endlicher Summen und Differenzen dargestellt. Das resultierende System simultaner, nicht-linearer, algebraischer Gleichungen wurde durch Iteration mit Hilfe der Newton–Raphson-Methode gelöst.

Ein neuer dimensionsloser Parameter wird vorgeschlagen; er charakterisiert die Gesamtwärmeabgabe eines Rippensystems mit gegenseitiger Zustrahlung. Seine Verwendung zeigt gegenüber dem herkömmlichen Rippenwirkungsgrad Vorteile bei der praktischen Gestaltung.

Für einen weiten Bereich von Emissionsverhältnissen und Zustrahlungen aus dem Raum wurden Rippen trapezförmigen, dreieckigen und rechteckigen Querschnitts untersucht. Die Rippenabmessungen und deren optimale Anzahl wurden bestimmt und Tabellen für die Abgabeleistung angegeben. Diese Analyse liefert auch einen, für den Vergleich von Rippenmaterialien unterschiedlicher Wärmeleitfähigkeit und Dichte zweckmässigen Ausdruck. Für eine vorgegebene Materialmenge ändert sich die Maximalwärmeabgabe mit $(k/\rho)^{1/3}$ bei konstanten anderen Faktoren.

Аннотация—В статье рассматриваются методы достижения максимальной теплоотдачи с помощью системы продольных ребер трапециевидного профиля при взаимной ирадиации. Конструктивное решение заключается в симметричном расположении ребер вокруг равномерно нагретого цилиндра с малым основанием. Уравнение температурного поля вдоль ребер сформулировано в виде конечных сумм и конечных разностей. В результате получена система совместных нелинейных алгебраических уравнений, решенных методом итераций Ньютона-Рафсона. Для характеристик теплоотдачи системы ребер с взаимным облучением предложен новый безразмерный параметр. Он более удобен для расчета, чем обычно применяемая эффективность ребер.

Трапецоидальные ребра, включая ребра треугольного и прямоугольного профиля, исследованы в широком диапазоне излучательных способностей и случайных пространственных радиаций. Определены оптимальное число ребер и соотношения их размеров. Представлены графики интенсивности теплообмена. В результате такого анализа получено выражение для сравнения ребер, изготовленных из материалов различной теплопроводности и плотности. При постоянной общей массе материала максимальное рассеяние тепла зависит только от величины k/ρ.